



# Application of borehole camera technology in the identification of an instantaneous strain-structural-plane slip rockburst

Haosen Guo<sup>1,2</sup> · Li Chen<sup>1</sup> · Jinyang Zhu<sup>1</sup> · Qiancheng Sun<sup>2,3</sup> · Yaxun Xiao<sup>3</sup>

Received: 29 June 2021 / Accepted: 13 March 2022 / Published online: 18 April 2022  
© Springer-Verlag GmbH Germany, part of Springer Nature 2022

## Abstract

The prediction of instantaneous strain-structural-plane slip rockbursts in deep-buried hard rock tunnels is a complex problem needing to be solved. An engineering case with a burial depth of 2375 m was taken for in situ testing. The structural plane distribution in surrounding rock was visualized, and the dominant influence of structural planes in the formation of rockbursts was discussed. Results showed that when the sidewall of tunnel is parallel to the structural plane developed in the surrounding rock or intersects the structural plane at a small angle (less than 30°), the instantaneous strain-structural plane slip rockburst risk is higher and the dominant position of structural plane is obvious. The evolution of rock mass fractures in rockburst-affected zones is demonstrated by the expansion of primary fractures, and no new fractures are generated. Different distributions of structural plane in surrounding rock provide different energy accumulation environments for rockburst incubation. The results offer a reference to the rockburst estimation and prediction, which has important theoretical value and engineering significance.

**Keywords** Deep tunnel · Hard rock · Rockburst · Structural plane · Borehole camera

## Introduction

A rockburst is a dynamic phenomenon, in which the elastic strain energy accumulated in an underground engineering rock mass is released suddenly under excavation or other

external disturbance, resulting in the bursting and ejection of the rock mass. As reported, a rockburst is characterized by suddenness, randomness, and danger (Fan et al. 2019; Du et al. 2020; Sepehri et al. 2020). Panic accompanies the progress of a rockburst, because they are difficult to predict, so often cause casualties, which seriously affect the construction of deep underground engineering works. Therefore, the establishment of a rockburst prediction and early warning system is a focus of much research into deep underground engineering (Song et al. 2017).

A series of rockburst prediction and early warning methods have been developed in the long-term practice of underground engineering (Zhou et al. 2018; Wang et al. 2018, 2020; Hu et al. 2020; Sainsbury and Kurucuk 2020; Kuang et al. 2021; Yu et al. 2020). The methods fall into two categories: single-factor criteria and multi-factor comprehensive criteria. The former includes various indicators proposed by scholars, such as elastic deformation energy index  $W_{et}$ , rock brittleness index  $K_u$ , linear elastic energy  $W_e$ , energy storage and consumption index  $K$ , stress index  $S$ , rockburst strength coefficient  $W$ , surrounding rock type, Russense criterion (Russenes 1974), and rockburst risk index (Dou et al. 2012). Multi-factor comprehensive criteria take more than two influencing factors into consideration simultaneously, for example, a microseismic method, established by Feng

---

✉ Qiancheng Sun  
qc\_sun@ctgu.edu.cn  
Haosen Guo  
guohaosen1988@126.com  
Li Chen  
chenwen1995730@qq.com  
Jinyang Zhu  
3307705108@qq.com  
Yaxun Xiao  
yxxiao2010@gmail.com

<sup>1</sup> East China Jiaotong University, Nanchang 330013, People's Republic of China

<sup>2</sup> Key Laboratory of Geological Hazards on Three Gorges Reservoir Area (China Three Gorges University), Ministry of Education, Yichang 443002, People's Republic of China

<sup>3</sup> State Key Laboratory of Geomechanics and Geotechnical Engineering, Institute of Rock and Soil Mechanics, Chinese Academy of Sciences, Wuhan 430071, Hubei, People's Republic of China

et al. (2015) for dynamic warning of rockburst development processes, and the rockburst tendency index RIV as established by Qiu et al. (2011), consider the stress control factor, a petrophysical property factor, rock mass system stiffness factor, and geological structure factor. Similarly, Huang et al. (2014) proposed the use of a multi-index evaluation method of rockburst propensity for long, deeply buried tunnels, taking the strength brittleness coefficient, deformation brittleness coefficient, elastic strain energy index, and tangential stress into account. The development of rockburst criterion has developed from use of single-factor criteria to multi-factor comprehensive criteria. In practical applications, the single criterion indicates the correct forecast trend with larger discreteness for individual data; the deviation of the results of predictions of rockbursts is caused by many factors. A comprehensive criterion is relatively accurate, but correlation analysis of multiple factors is complex, and hence showed limited utility. Therefore, the establishment of a high-performance rockburst prediction and early warning system is inseparable from the accurate determination of the factors affecting rockburst risk, which are crucial to the accuracy and efficiency of rockburst prediction methods.

Engineering practice shows that the prevailing stress field and rock mass condition play dominant roles in the occurrence of a rockburst, where the stress field conditions include the initial stress state in the rock mass and the degree of influence of the method of excavation on the stress distribution; the condition of the rock mass includes its mechanical properties and geological structure. Feng et al. (2022) compared the similarities and differences between deep parallel tunnels with alternating soft-hard strata. Instantaneous rockbursts can be divided into strain-type rockbursts and structural rockbursts. Different dominant factors need to be considered for different types of rockburst. The strain-type rockburst is mainly controlled by the stress field conditions. Accurately determining the initial stress field state and excavation conditions would help achieve better prediction and early warning of strain-type rockbursts.

For deep hard-rock tunnels with a small range of disturbance, in high-strength rock of good integrity, it is easy to induce a structural rockburst when Grade IV or V structural planes around the tunnel have certain mechanical properties and meet certain geometric conditions (Liu et al. 2018a, b; Feng et al. 2020, 2019). At present, a rockburst prediction criterion is established based mainly on the in situ stress, rock strength, rock brittleness, and burial depth; although the proposed strain-structural-plane sliding rockbursts thus predicted are rare, the impact of structural planes on the generation of rockbursts warrants further study. Therefore, the in situ test results from a strain-structural-plane-sliding-type rockburst were analyzed based on the tunnel excavation required for a deep underground laboratory. By comparing the structural plane distribution between the rockburst

occurring in one tunnel with another, combined with the numerical simulation results, the elastic strain energy distributions of rock mass under different structural plane conditions are summarized, revealing the dominant influence of the structural plane distribution on the process of rockburst evolution in a deep hard-rock tunnel.

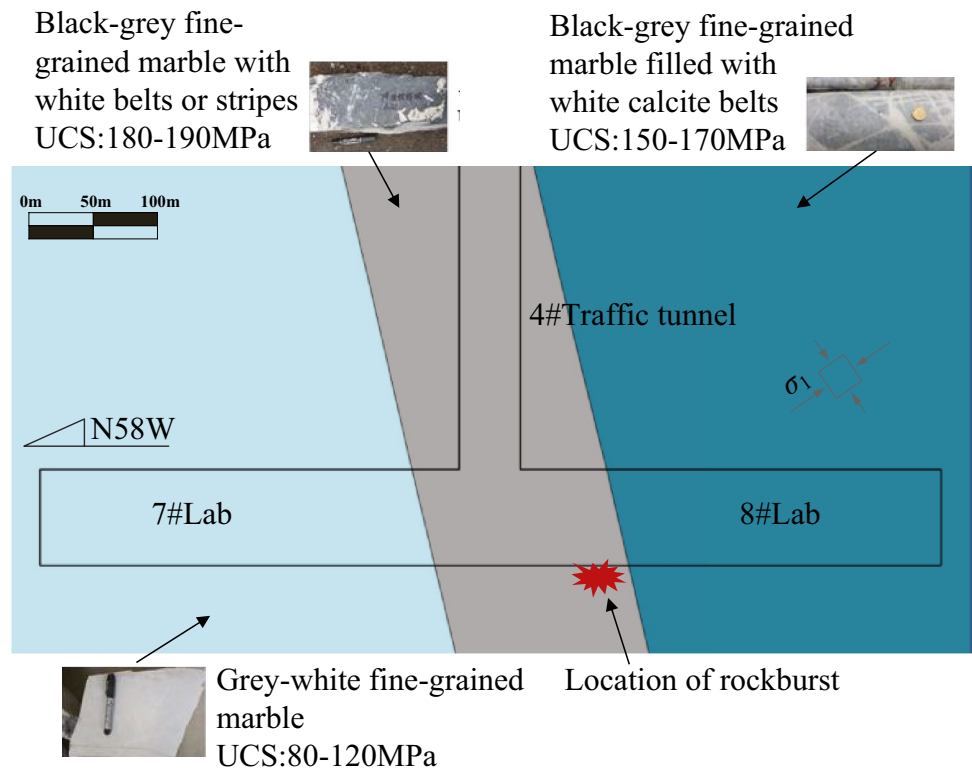
## Overview

An underground laboratory at a depth of 2375 m, in which geostatic stresses dominate the stress field, is located in the landform slope zone between the Sichuan Basin and the Qinghai-Tibet Plateau. The lithology of the strata along the cavern exposed mainly grey-white fine-grained marble, black-grey fine-grained marble with white belts or stripes, and black-grey fine-grained marble filled with white calcite belts (Fig. 1); this was classified as a typical deep hard-rock tunnel. The laboratory with a cross-section of 14 m × 14 m was excavated by drilling and blasting method, which was divided into three steps (middle guide tunnel excavation, upper expansion excavation, and bottom excavation) and the supporting method relied on bolting and shotcrete.

During the excavation of the middle guide tunnel of the No. 8 laboratory, an extremely strong rockburst with a blast depth of 3.3 m occurred; the total length of the affected area was nearly 44 m. The damage location is shown in Fig. 1. After detailed geological investigation, three groups of structural planes were exposed in the rockburst area, in which two groups of the No. 1 structural plane lay approximately parallel to the direction of excavation, while the No. 2 structural plane intersected the tunnel wall at a small angle, forming the boundary of the blasting crater. Two groups of No. 3 structural planes further from the explosion pit are approximately perpendicular to the excavation direction. According to the relative position of the blasting pit and the structural plane, it can be confirmed that this structural rockburst was controlled by the structural planes.

The experimental method of rockburst tendency index  $W_{et}$  (Liu et al. 2017), which is the most widely used for rockburst propensity evaluation, using the ratio of elastic deformation energy  $\Phi_{SP}$  and the plastic deformation energy  $\Phi_{ST}$ , namely,  $W_{et} = \Phi_{SP} / \Phi_{ST}$ , was adopted to conduct the rockburst tendency test on the marble with T<sub>2b</sub> grey-white lithology and local white band-like fine crystals coming from the laboratory area. Table 1 shows the calculated results of the rockburst tendency index. According to the method, the four interval divided by 2.0, 3.5, 5.0 of  $W_{et}$  means no rockburst, light rockburst, medium rockburst, and heavy rockburst, respectively. The rockburst tendency index  $W_{et}$  in the laboratory indicated low or medium rockburst risk, while the fact of the extremely strong rockburst in the No. 8 laboratory could prove the failure of this method in the laboratory cave area, which revealed

**Fig. 1** Prevailing geological conditions



that rockburst gestation is not only related to the prevailing lithology.

To clarify the role of geological structure in inducing the extremely strong rockburst in the No. 8 laboratory, borehole digital camera technology was adopted in the process of in situ observation of the rockburst site. By comparing the lithology, tunnel buried depth, initial stress field, tunnel excavation method, and tunnel size in the rockburst area and the safe-passage tunnel, the distribution of the internal structural plane of the surrounding rock, obtained by digital camera, revealed the environment around, and leading to, this rockburst.

### Analysis of borehole digital camera test

#### Test equipment and scheme

The panoramic borehole digital camera was used for comprehensive inspection, photographing, video recording and

imaging of drilling holes with high accuracy and a simplicity of operation. Such devices are often used to observe the development of macroscopic fractures in surrounding rock. The distribution of the fissures in the borehole was obtained by the use of the panoramic digital camera, and the test results of multiple boreholes in the same direction with proper spacing can be used to visualize the distribution of structural planes in the surrounding rock.

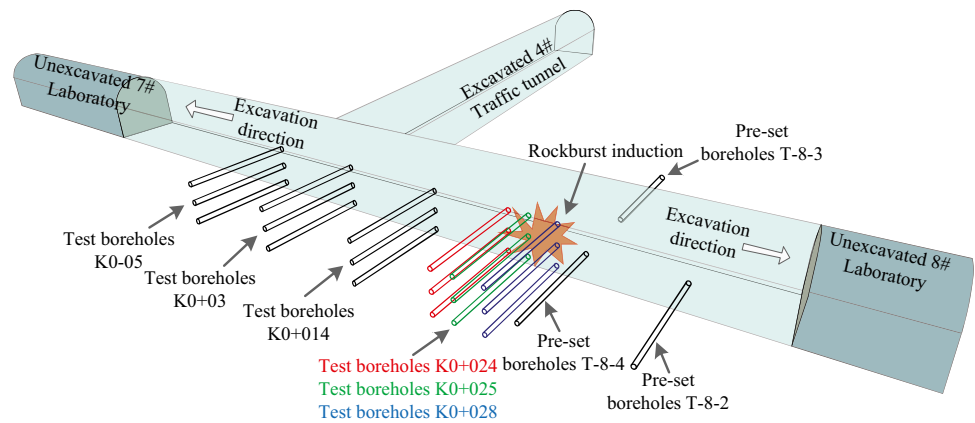
As shown in Fig. 2, three pre-set boreholes (T-8-2, T-8-3, T-8-4) and six groups of test boreholes at chainages K0-05, K0+03, K0+014, K0+024, K0+025, and K0+028 were located in the surrounding rock. The preset boreholes T-8-2, T-8-3, and T-8-4 had been arranged before the rockburst, and several borehole-camera surveys were undertaken. K0+024, K0+025, and K0+028 were arranged in the rockburst area, K0+024 and K0+028 were arranged on the left and right edges of the rockburst area, and K0+025 was arranged in the blast hole (Fig. 3).

Based on the ductility of the structural plane, these boreholes can help to map the detailed distribution of the structural planes in the rock surrounding the rockburst area, while boreholes K0-05, K0+03, and K0+014, arranged in the safe passage tunnel, provided the structural plane distribution. According to the occurrence of fissures and fracture trend as evinced by borehole camera footage, we could judge whether the visible crack extended to the adjacent borehole, giving the spatial distribution of structural planes in the surrounding rock (Fig. 4).

**Table 1** Calculated results of rockburst tendency index

Test number	$W_{et}$	The average	Risk of rockburst
1	3.82	3.59	Low or moderate
2	2.98		
3	3.54		
4	3.25		
5	4.38		

**Fig. 2** Layout of borehole for rock structural plane observation



### Fracture evolution tests before and after the rockburst

Borehole camera surveys were conducted in boreholes T-8-2, T-8-3, and T-8-4 (Fig. 5) on 13 and 25 August, the final survey being two days after an extremely strong rockburst occurred near those boreholes on 23 August.

The distances from boreholes T-8-2 and T-8-3 to the rockburst pit were 12.6 m and 14.5 m, respectively. There was only a very small amount and extent of primary cracking opening or closing therein (Fig. 6(a), (b)). The borehole T-8-4 is 1.6 m from the rockburst pit: obvious primary fracture expansion occurred after the rockburst. This showed that the expansion of primary fractures linearly decreased along the borehole depth, without any new fracture generation (Fig. 6(c)). It can then be inferred that the strong disturbance caused by rockburst event has no obvious effect on rock mass fractures 12.6 m away. The influence of the rockburst on the surrounding rock was manifest as the expansion of primary fractures but no new fractures. The occurrence

of the rockburst had no effect on the spatial distribution of structural planes in the surrounding rock.

### Fracture distribution test in the rockburst zone and safe passage tunnel

#### Test results: the safe passage tunnel section

The K0-05 borehole camera test results show that there are three parallel structural planes developed in the surrounding rock. The second is at a large spacing and with filling material within its layers, while the angle between the structural plane and the side wall of the tunnel is  $35^\circ$  to  $40^\circ$  (Fig. 7(b)).

The K0+03 borehole camera test results show that there are two large structural planes in the surrounding rock: the width of the fractures is large, but they contain no infilling material. The angle between the structural planes which is closer to the side wall of the tunnel is between  $30^\circ$  and  $35^\circ$  (Fig. 7(c)).

The K0+14 borehole camera test results show that there are four structural planes in the side wall of tunnel, two of which were closer to the tunnel side wall opened but were without infilling material, intersected the sidewall at an angle of  $30^\circ$  to  $35^\circ$ , while another two structural planes formed at greater distance were quasi-parallel to the side wall (Fig. 7(d)).

The borehole camera test results from sections K0+024, K0+025, and K0+028 show that there are four groups of structural planes developed in the surrounding rock around the rockburst. The exposed structural planes 1#, 2#, 3#, 4# in rockburst area are shown in Fig. 8. Influenced by rockburst, a huge number of fracture zones were developed at K0+025, and the surrounding rock collapsed into the borehole. Measuring data showed that the intersection angle between side-wall of the tunnel and structural plane, which dominated the occurrence of this rockburst, is small and almost parallel (Fig. 8).

In this engineering case, comparative analysis found that the aforementioned three safe passage tunnel sections also

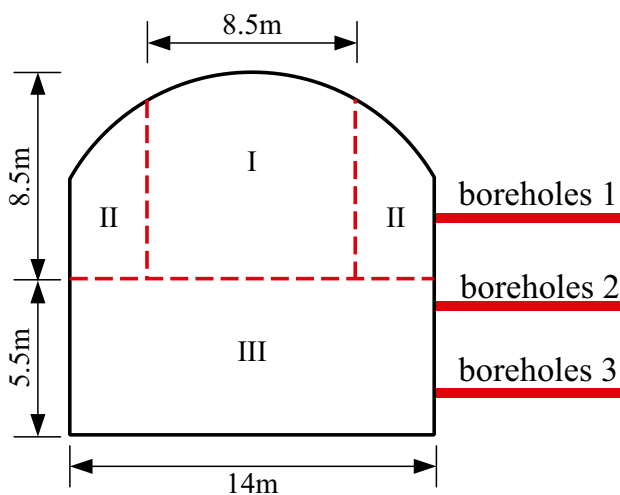
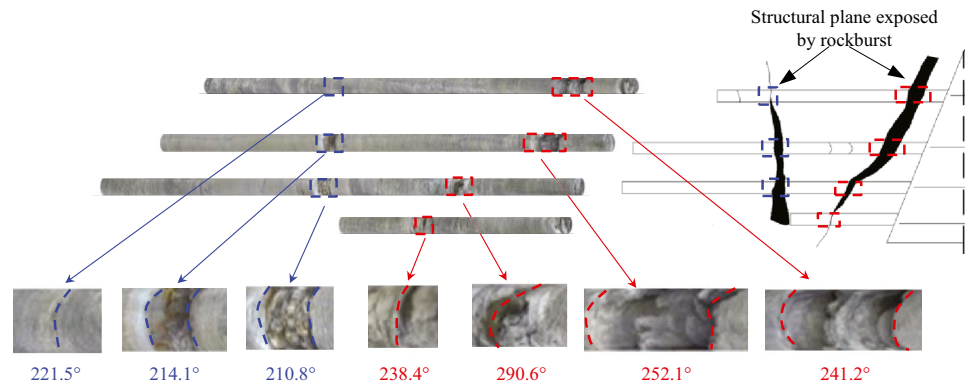


**Fig. 3** Distribution of boreholes in the test section



**Fig. 4** Acquisition of the internal fracture distribution in borehole K0+03



developed structural planes and the tunnel sidewall angles of intersection therewith are larger (exceeding  $30^\circ$ ); however, structural planes were almost parallel to the tunnel sidewall in the rockburst section. This showed that, for deep hard-rock tunnels with a mainly geostatic initial stress field, a higher rockburst risk arose when the angle between the inner structural plane of surrounding rock and the sidewall of tunnel is smaller (less than  $30^\circ$ ).

As reported, the occurrence of a rockburst is the result of elastic strain energy accumulation (Manouchehrian and Cai 2018). The sporadically developed structural plane in the surrounding rock would cause a discontinuity in the distribution of stress and strain energy, resulting in a high strain-energy accumulation. If enough elastic strain energy aggregated in the surrounding rock, once the rock mass became unstable, the damage will be severe, and a large amount of elastic strain energy would be released in the form of kinetic energy, characterized by rock mass ejection, resulting in a rockburst. To verify this conjecture, a numerical model of an engineering case study was established to study the energy characteristics in the excavation unloading process.

### Energy characteristic analysis

The triaxial testing to simulate the high-stress unloading process of marble showed that the elastic strain energy accumulated in the surrounding rock was directly related to the maximum principal stress difference (Fig. 9). The accumulation of elastic strain energy can be judged by the maximum principal stress difference (Zhang et al. 2021). Calculation of the elastic strain energy accumulated in the surrounding rock can be used to judge the risk of a rockburst at a macro-scale perspective. We aimed to study the dominant influence of structural planes in the development of a rockburst in the above case, and to assess the influence of the angle between different structural planes and the side wall on the elastic strain energy distribution in the surrounding rock. To achieve these purposes, the scenario could be simplified to a plane strain problem considering the longitudinal direction of the tunnel and the change in the angle between the structural plane and the side wall on the section of the tunnel.

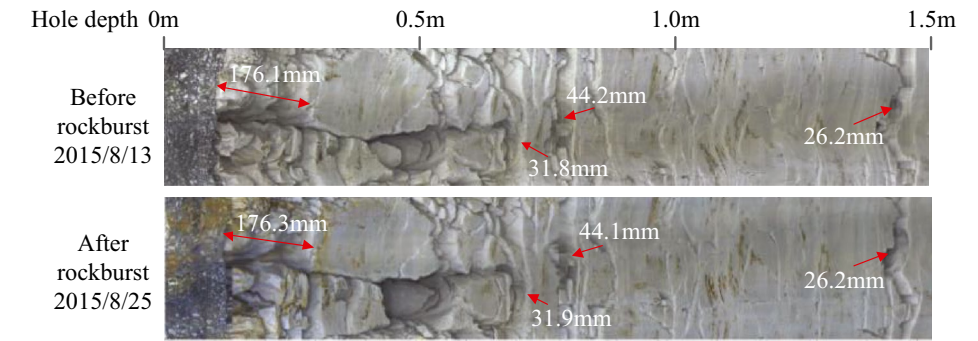
A model with a width and height of 140 m (Fig. 10) was established by Flac3d, which is commonly used finite difference method in geotechnical numerical simulation, to obtain the elastic strain energy distribution in the rock mass after excavation. The Mohr–Coulomb elastic–plastic model (Liu et al. 2018a) was used considering the in situ stress state. Back analysis of rock mass stress conditions was conducted based on the deformation and plastic zone of rock mass after excavation; the stress parameters of the rock mass were obtained from intelligent parameter inversion as shown in Table 2. The boundary conditions on the model were such that normal constraints on the bottom, and the normal stress applied to the left, right, and top were 47.86 MPa, 47.86 MPa, and 62.19 MPa, respectively.

The simulation of the native cracks in the rock mass refers to the literature (Feng et al. 2018), and the mesh strength at the cracks within the rock mass is weakened appropriately to simulate native cracks existing within the surrounding rock. Three types of working conditions were considered: (1) structural planes at a  $45^\circ$  intersection in the tunnel sidewall

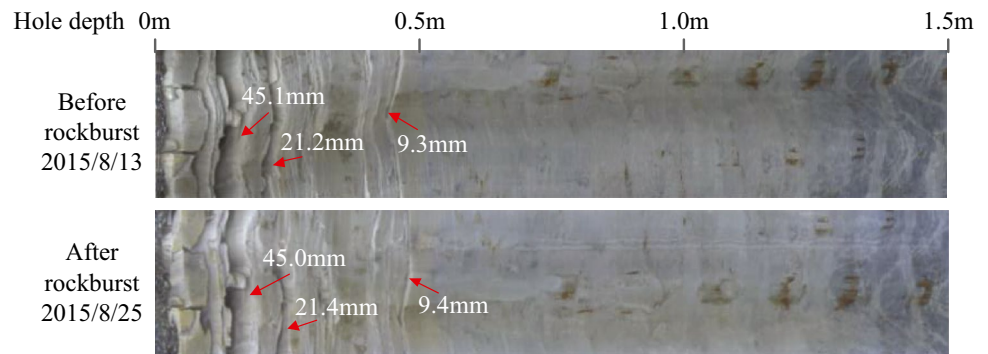


**Fig. 5** Boreholes T-8-2, T-8-3, and T-8-4 around the rockburst pit

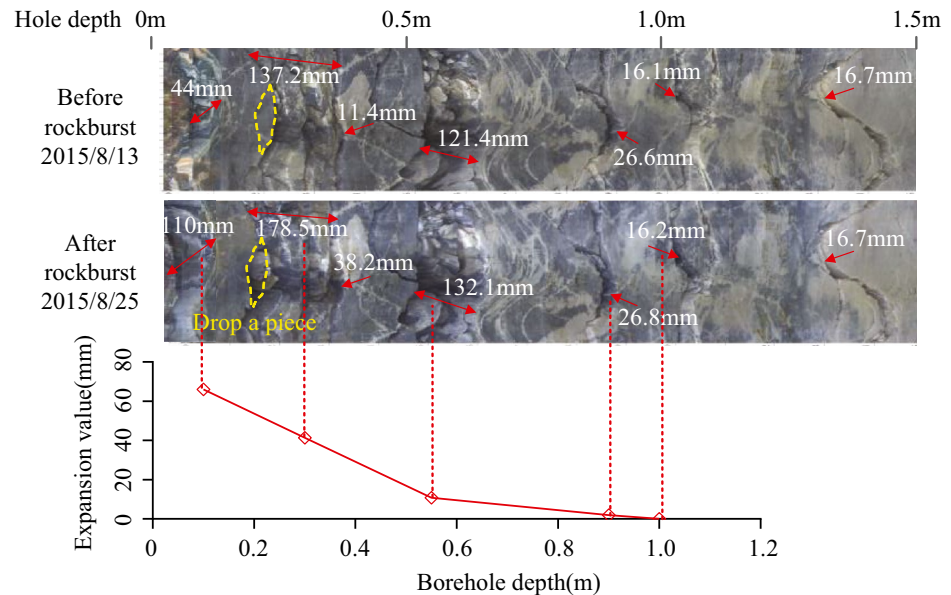
**Fig. 6** Test results: T-series pre-set boreholes before and after rockbursting



**(a)** Camera results of boreholes T-8-2



**(b)** Camera results of boreholes T-8-3



**(c)** Camera results of boreholes T-8-4

(Fig. 11(a)); (2) structural planes at a 20° intersection in the tunnel sidewall (Fig. 11(b)); and (3) structural planes parallel to the tunnel sidewall (Fig. 11(c)). By sampling the complete marble rock mass and the rock mass containing joints, true triaxial test was performed to obtain the parameters for each material (Table 3).

The maximum principal stress differences after excavation under different working conditions are shown in Fig. 11. Based on the direct relationship between the maximum principal stress difference and the elastic strain energy stored in surrounding rock, the distribution of elastic strain energy can be observed. The maximum elastic strain energy is located at

**Fig. 7** Borehole camera test results in the safe passage tunnel

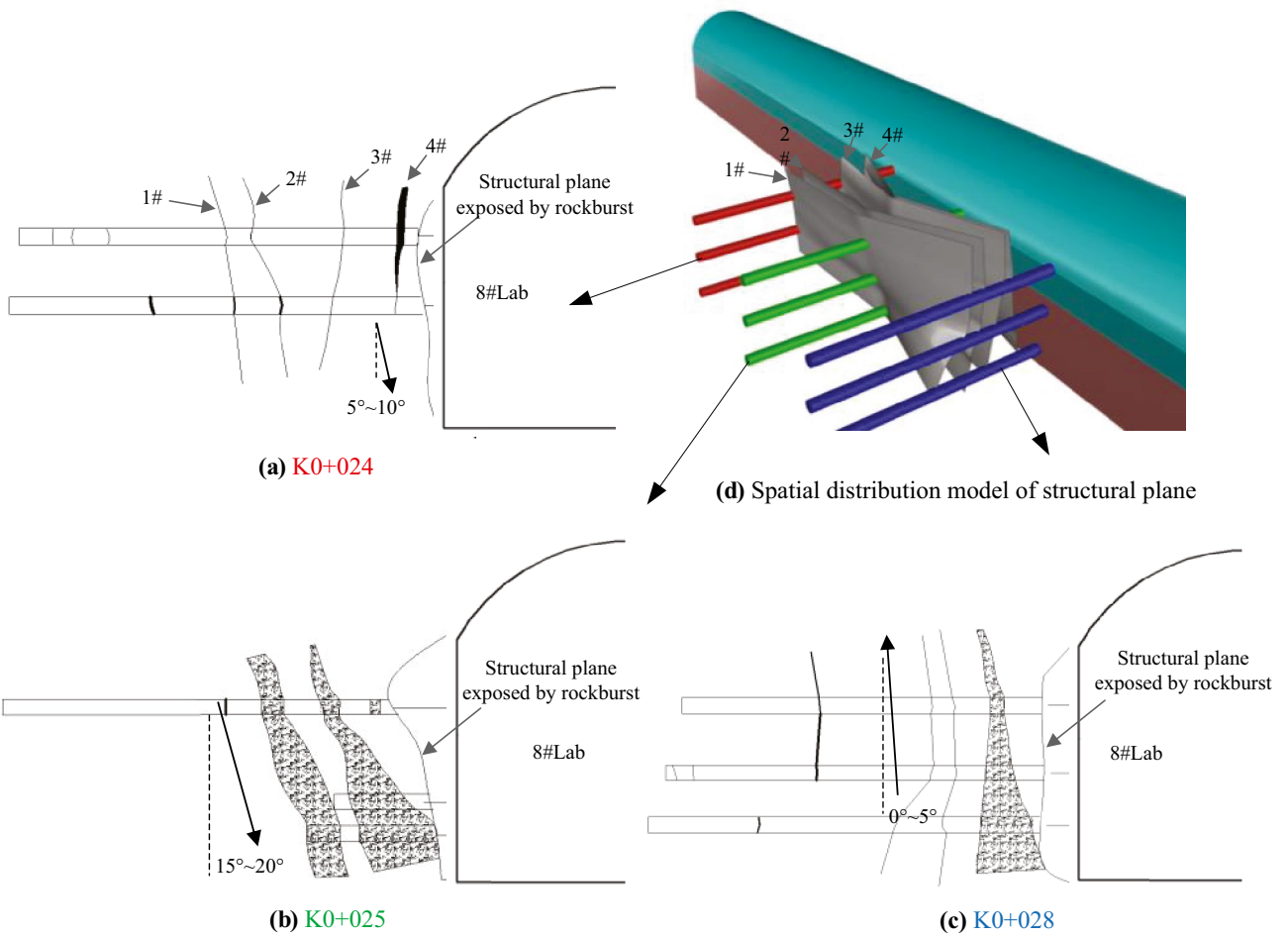
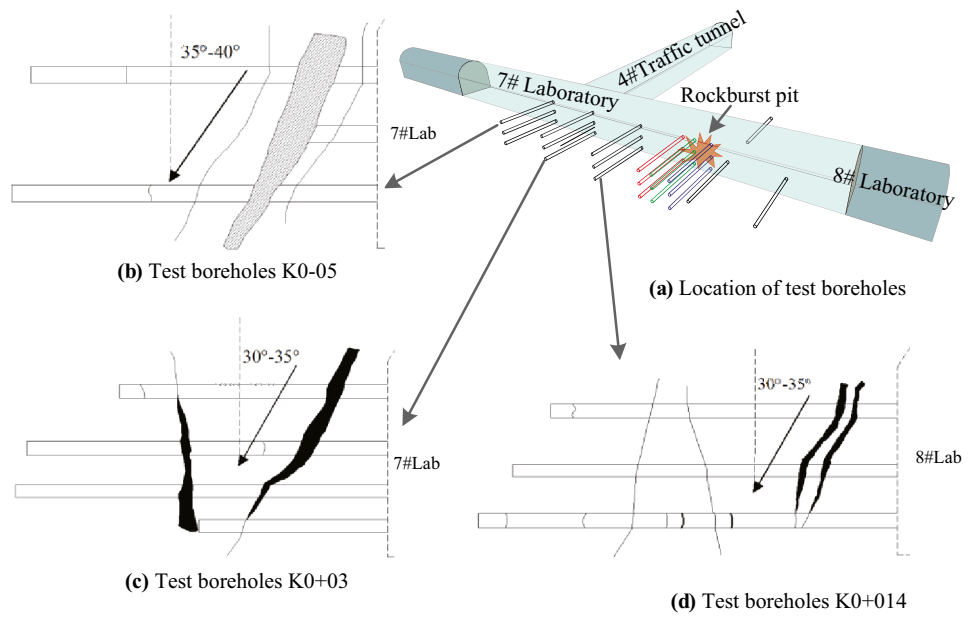


**Fig. 8** Borehole camera test results in the rockburst tunnel section



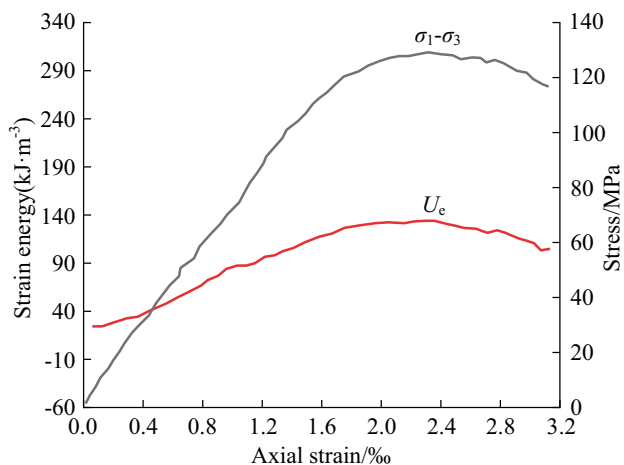


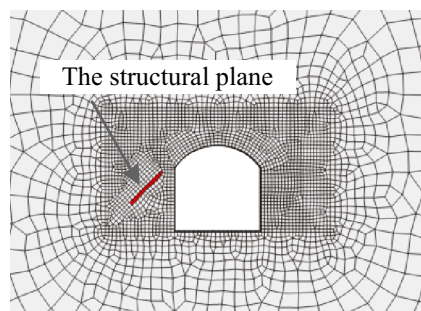
**Fig. 9** The maximum principal stress difference and elastic strain energy for marble specimens under unloading confining pressure with high triaxial stress (Huang et al. 2012)

the shoulders and feet to both the left and right. The elastic strain energy in the sidewall of the tunnel is lower without structural planes in the surrounding rock. The presence of the structural plane pushes the zone of accumulation of elastic strain energy to greater depth in the surrounding rock when the angle between the structural planes and the sidewall of the tunnel is large (Fig. 11(a)). Because the structural planes in rock mass is the uncoordinated deformation area for stress adjustment, when set the distance between structural plane and the sidewall as constant, the bigger the intersection angle is, the smaller component of the elastic strain energy stored in the structure plane vertical to the sidewall is, and the elastic strain energy component oriented along the structure is greater. Under the action of maximum principal stress, the strain oriented inward develop along the structure plane deep rock mass rather than extending outward to the sidewall. When a set of structural planes lies parallel to the sidewall of the tunnel, an elastic strain energy accumulation zone, which connected the areas of the tunnel shoulder, side wall and the tunnel feet, formed as shown in Fig. 11(c).

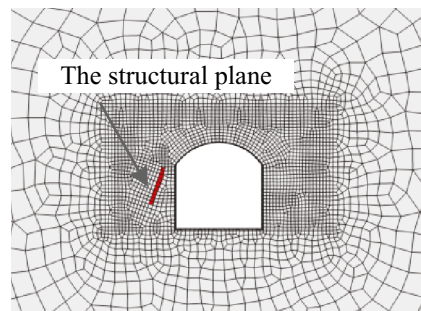
The simulated testing of a structural plane shows that when the shear stress on the structural plane under excavation disturbance is in critical state, the surrounding rock readily slips and fails, causing a rockburst. The maximum shear stress  $\tau_{max}$  under triaxial compression of the surrounding rock can be obtained directly as follows:

$$\tau_{max} = \frac{\sigma_1 - \sigma_3}{2}$$

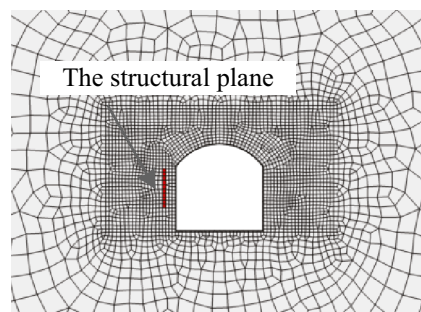
Figure 11 shows that the angle between the structural plane and the sidewall of tunnel has a significant effect on the distribution of the maximum shear stress: the zone of



**(a)** 45° between structural plane and the sidewall of tunnel



**(b)** 20° between structural plane and the sidewall of tunnel



**(c)** The structural plane is parallel to the sidewall of tunnel

**Fig. 10** Numerical model of different structural plane distributions

accumulation of high elastic strain energy after excavation and unloading is under a higher shear stress in this case.

According to the test analysis of fracture development and the calculated stress distribution, the incubation process of instantaneous strain-structural plane sliding type rockbursts (in this practical case) can be summarized thus:

- (1) Several structural planes parallel to the sidewall of the tunnel are sporadically developed in the rock surrounding the rockburst area before excavation. When exca-

**Table 2** Initial geo-stress state in the numerical modelling

$\sigma_x$ (Mpa)	$\sigma_y$ (Mpa)	$\sigma_z$ (Mpa)	$\tau_{xy}$ (Mpa)	$\tau_{yz}$ (Mpa)	$\tau_{zx}$ (Mpa)
47.86	54.55	62.19	4.52	2.35	15.14



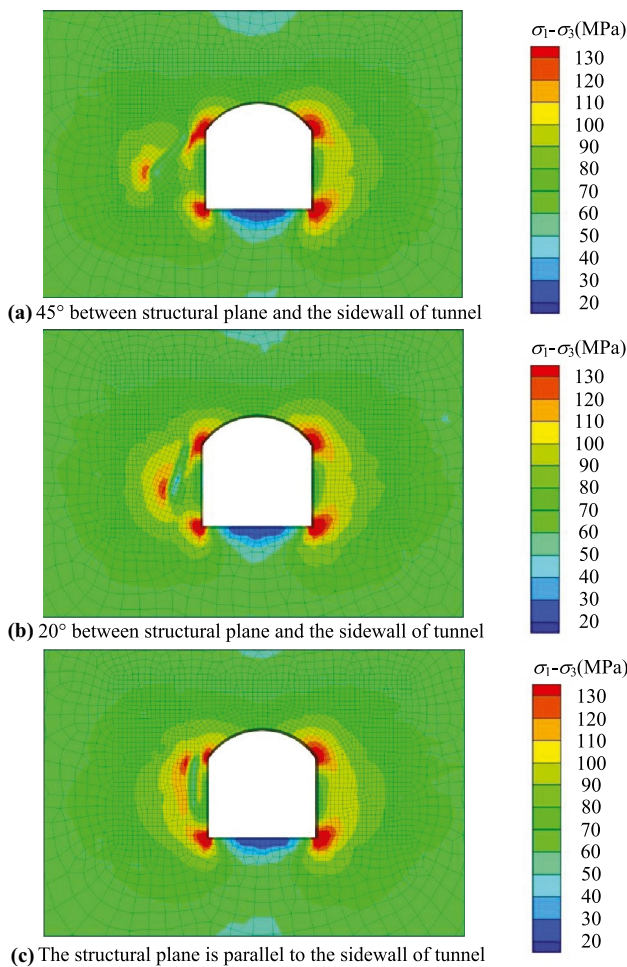


**Fig. 11** Maximum principal stress difference distribution with different structural planes in the surrounding rock

vated near the structural planes, the structural planes are mobilized under the action of the secondary stress field (Fig. 12(a));

- (2) During the adjustment of the stress field caused by excavation and unloading, the initiation of new cracks and the expansion of primary cracks appeared in the rock surrounding the tunnel (Fig. 12(b));
- (3) The elastic strain energy in the surrounding rock between the structural plane and the sidewall of tunnel increased during adjustment of the geo-stress field, exerting a greater shear stress on the structural plane, and the cracks near the structural plane developed in a particularly intense manner, and gradually delineated the potential range of the eventual rockburst (Fig. 12(c));

- (4) The rockburst body slips and fails under excavation-induced disturbance. Part of the elastic strain energy stored in the rockburst body is dissipated in overcoming the resistance of the rock masses on both sides: the remaining energy is released in the form of kinetic energy, which is manifest as a rapid ejection of rock. The blasting pit is exposed along the structural surface (Fig. 12(d)).

The simulation and in situ photograph (Fig. 13) validated the aforementioned stages: the outline of the rockburst failure area is consistent with the outline of the elastic strain energy accumulation zone in Fig. 12(d).

### Statistical analysis of instantaneous strain-structural-plane type rockburst

As reported, the SK8 + 200 to 8 + 800 section of the drainage tunnel at Jinping II Hydropower Station is a typical deep hard-rock tunnel, with a minimum burial depth of 2393 m and a maximum burial depth of 2523 m. The lithology of the surrounding rock is white thick marble of the BaiShan Formation. A TBM was used for full-face excavation over a 7.2-m excavation diameter. During excavation, this section is highly prone to rockbursts. Zhao et al. (2019) reported all rockburst events in this typical section of rockburst. Through statistical analysis of the grades of rockburst events and the occurrence of structural plane exposed by the rockburst pits (Table 4), it was found that 13 out of 15 rockbursts exposed the structural plane, with the angles between the structural plane and the sidewall being less than 30°, and the rockbursts gathered mostly in the sidewall of the tunnel or expanded to the spandrel, indicating that the incubation of the rockburst was strongly dominated by the internal structural planes in the surrounding rock.

The aforementioned statistical analysis was consistent with in situ observations and numerical simulation of the engineering case, that is, when the angle between the internal structural surface and the sidewall of the tunnel to be excavated is small, it was conducive to the incubation of a rockburst. The influence of rockburst accidents on engineering operations can be reduced to a certain extent by making the tunnel sidewall intersect the dominant structural plane in surrounding rock at a large angle (as far as possible), or taking the small angle intersection of the structural plane and the tunnel sidewall as the key area for implementation of rockburst prevention measures.

**Table 3** Parameters of physical and mechanical properties

Material	Modulus of elasticity/GPa	Poisson's ratio	Cohesive forces/MPa	The angle of internal friction/(°)
Original rock	29.2	0.2	35	30
Degraded rock mass	3.5	0.2	3	23

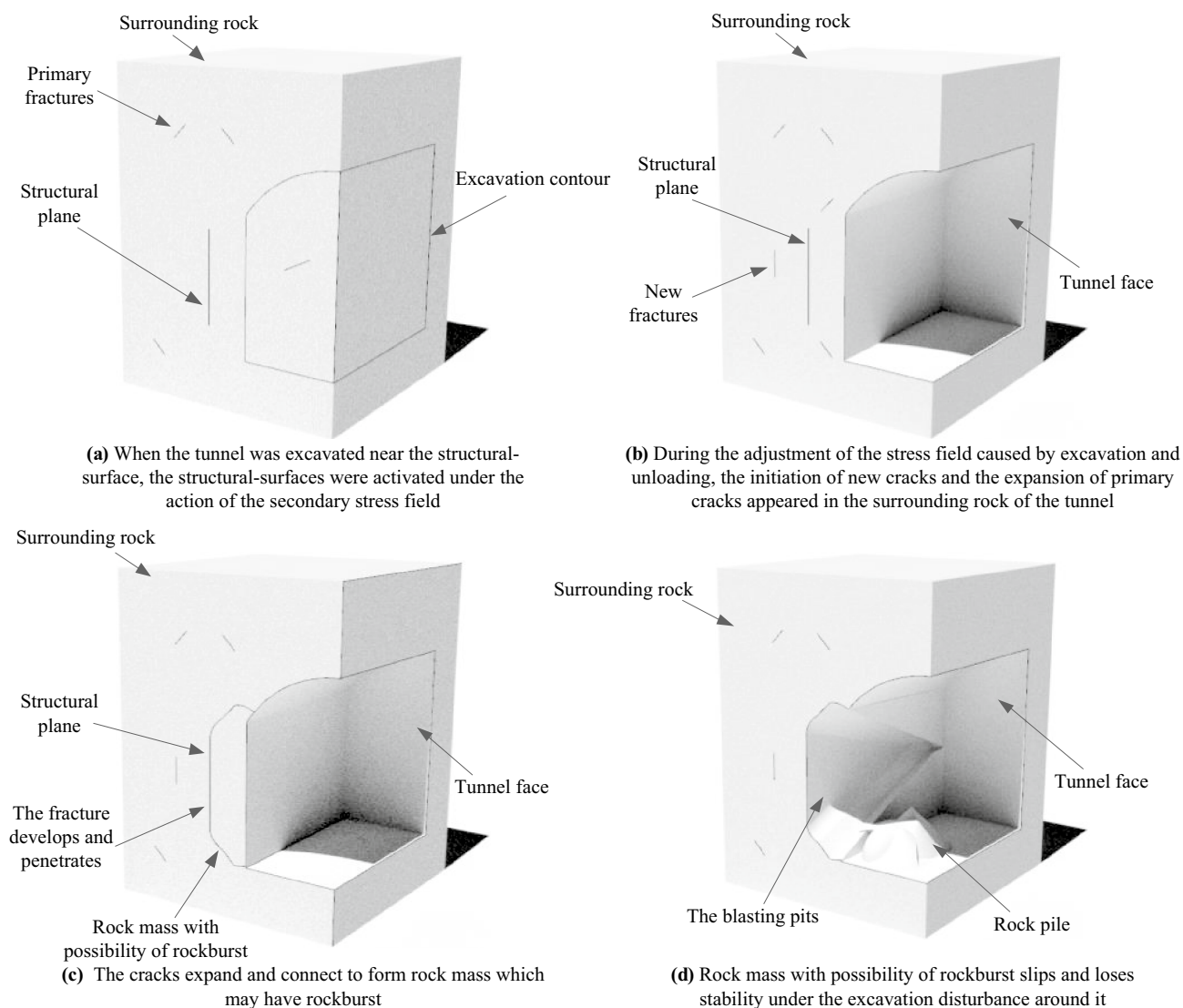


Fig. 12 Incubation process simulation of rockburst for the in situ engineering case

## Discussion

This study analyzed the same stress and lithological conditions and focused on the key role of structural planes running parallel to the sidewall of a tunnel or with a small intersection angle therewith. It is noteworthy that there are many factors affecting the development of a rockburst. The risk of a rockburst increases with a larger intersection angle between the tunnel and the structural planes. The following case shows a deep buried tunnel with black grains in monzonitic granite in which six groups of structural planes developed, of which three intersected the tunnel at between  $40^\circ$  and  $70^\circ$ . Five rockbursts occurred during construction of a pilot tunnel, and three of them occurred in the sections at DK194+625.4, DK194+632.9, and DK194+635.9 (Fig. 14). The case study analysis showed that the structural

types of rockburst are not only displayed along the structural plane to form rockburst pits, and when there is a very weak structural plane or space cutting formed unstable dangerous rock masses, the excavation-induced disturbance will trigger a rockburst, even though the elastic strain energy accumulation in the rock mass remained relatively low.

Even if, on the other hand, there is a structural plane parallel to sidewall, the distances from the structural plane to the sidewall, the geo-stress direction, etc., are the more important factors influencing elastic strain energy accumulation: these predicate the occurrence of a rockburst. Single-factor analysis was adopted, combined with in situ data collection from a field site, to discuss the dominant influence of the structural planes in the development of a rockburst. The effects of other factors in the development of a rockburst warrant further analysis by way of other engineering examples.

**Fig. 13** Photograph showing the actual rockburst

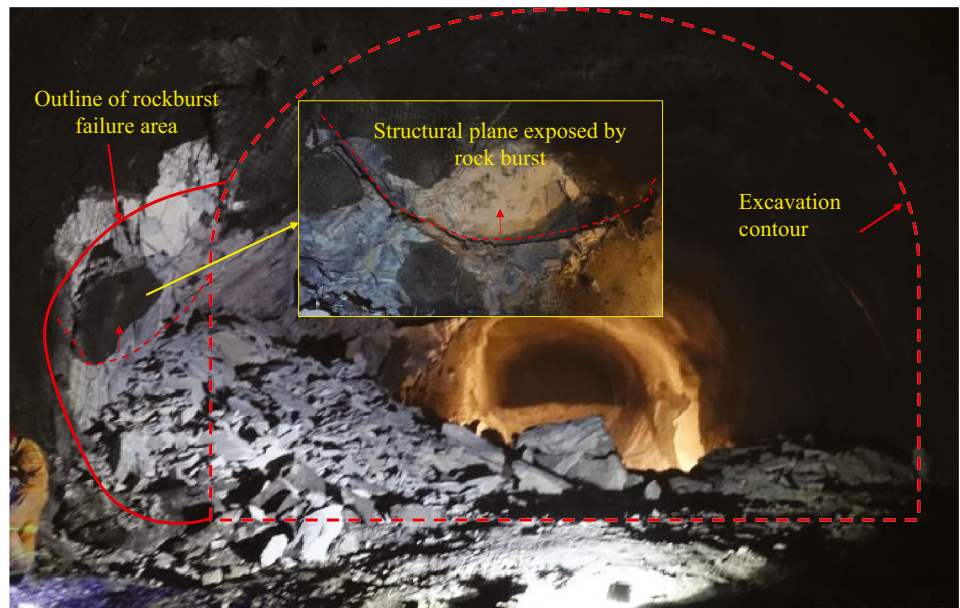
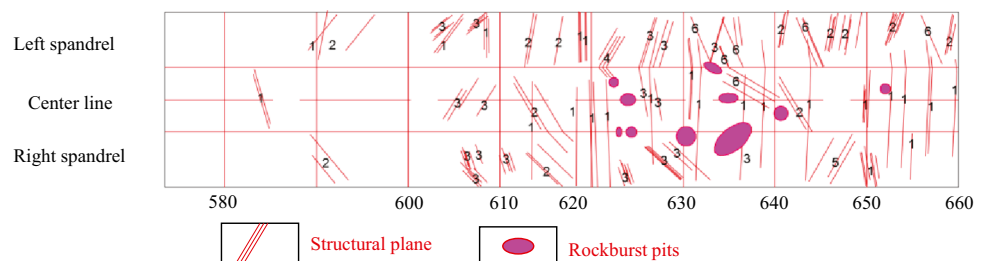


**Table 4** Rock mass structural plane and the occurrence of rockbursts at chainages SK8+200 to 8+800 in the drainage tunnel

No.	Rockburst pile no.	Location of the rockburst	Grade of rockburst	Angle between the structural plane and the sidewall
1	SK8+407~411	The south sidewall	Slight	5~15
2	SK8+440~445	Southside wall to arch shoulder	Slight	5~15
3	Sk8+462~468	The north sidewall	Slight	15~20
4	SK8+485~495	The north sidewall	The delay type of medium	25~30
5	SK8+501~508	The south sidewall	Slight	5~10
6	SK8+525~530	The south sidewall	Slight	5~10
7	SK8+555~558	The north sidewall	Slight	None
8	SK8+672~678	South sidewall to arch shoulder	Medium	5~10
9	SK8+703~709	South sidewall to arch shoulder	Strong	5~10
10	SK8+708~715	South sidewall to arch shoulder	Strong	5~10
11	SK8+717~732	South sidewall to arch shoulder	Strong	5~10
12	SK8+709~757	North sidewall to arch shoulder	Strong	5~10
13	SK8+742~757	South sidewall to arch shoulder	Medium	None
14	SK8+764~775	South sidewall to arch shoulder	Strong	20
15	SK8+767~782	North sidewall to arch shoulder	Medium	20

**Fig. 14** Location of rockbursts and distribution of structural planes during the excavation of a tunnel





## Conclusions

Compared the distribution of structural planes, as observed by drilling camera-inspection boreholes in the surrounding rock, between rockburst areas and a safe passage tunnel, the influence of structural planes in the surrounding rock on the induction of a rockburst was investigated, and the dominant influence of structural planes on the incubation of an instantaneous strain-structure plane type rockburst was further ascertained by simulation and analysis of a practical engineering case study. The main conclusions are as follows:

- (1) The occurrence of rockburst will not cause the initiation of cracks in the rock mass but will splay the primary fissures within the area thus affected. The test results pertaining to the fracture distribution after a rockburst can be used to speculate about the characteristics of the fracture distribution before the rockburst. The structural planes in the rockburst area are parallel, or intersect at a small angle, to the sidewall of the tunnel. The angles between the structural plane developed in the surrounding rock of the safe passage sections and the sidewall of the tunnel are all relatively large (exceeding 30°); the distribution of structural plane in the surrounding rock is a key factor affecting the development of extremely strong rockbursts in this case.
- (2) The different distribution patterns of structural plane in surrounding rock offer a different environment for energy accumulation. When the structural plane of the surrounding rock is parallel to the sidewall or intersects it at a small angle, it induces a higher risk of rockburst, caused by the high elastic strain energy accumulation zone and high shear stress accumulation zone in the structural plane and their location under excavation-induced disturbance. It is difficult to generate a consecutive rockburst area due to low elastic strain energy in the sidewall, when the angles between the structural planes in the surrounding rock and the sidewall of the tunnel are large, and even if the arch shoulders and feet of the tunnel are in a state of higher elastic strain energy, there is a very low probability of a rockburst occurring.
- (3) The existing state of the structural planes is the critical factor affecting the development of instantaneous strain-structural-plane type rockbursts. More than 90% of instantaneous strain-structural-plane type rockbursts occur in areas where the angle between the sidewall of the tunnel and the structural plane in surrounding rock is less than 30°. When the angle is large, the stress field and the spatial cutting of the structural plane are important factors affecting the development of a rockburst.

**Funding** This study was funded by the National Natural Science Foundation of China (Grant No. 51909136), the Natural Science Foundation of Jiangxi Province (Grant No. 20202BABL214051), and the Open Research Fund of State Key Laboratory of Geomechanics and Geotechnical Engineering (Grant No. Z018012), the Open Research Fund of the Key Laboratory of Geological Hazards in the Three Gorges Reservoir Area (China Three Gorges University) (Ministry of Education Grant No. 2020KDZ03).

**Data availability** The data used to support the findings of this study are available from the corresponding author upon request.

## Declarations

**Conflict of interest** The authors declare no competing interests.

## References

- Dou LM, Chen T, Gong S, He H, Zhang S (2012) Rockburst hazard determination by using computed tomography technology in deep workforce. *Safety Sci* 50(4):736–740. <https://doi.org/10.1016/j.ssci.2011.08.043>
- Du F, Wang K, Guo YY, Wang GD, Wang L, Wang YH (2020) The mechanism of rockburst-outburst coupling disaster considering the coal-rock combination: An experiment study. *Geomech Eng* 22(3):255–264. <https://doi.org/10.12989/gae.2020.22.3.255>
- Fan JY, Chen J, Jiang DY, Wu JX, Shu C, Liu W (2019) A stress model reflecting the effect of the friction angle on rockbursts in coal mines. *Geomech Eng* 18(1):21–27. <https://doi.org/10.12989/gae.2019.18.1.021>
- Feng F, Li XB, Rostami J, Li DY (2019) Modeling hard rock failure induced by structural planes around deep circular tunnels. *Eng Fract Mech* 205:152–174. <https://doi.org/10.1016/j.engfracmech.2018.10.010>
- Feng GL, Chen BR, Xiao YX et al (2022) Microseismic characteristics of rockburst development in TBM tunnels with alternating soft–hard strata and application to rockburst warning: A case study of the Neelum–Jhelum hydropower project. *Tunn Undergr Space Technol* 122:104398. <https://doi.org/10.1016/j.tust.2022.104398>
- Feng GL, Feng XT, Chen BR et al (2015) A microseismic method for dynamic warning of rockburst development processes in tunnels. *Rock Mech Roch Eng* 48(5):2061–2076. <https://doi.org/10.1007/s00603-014-0689-3>
- Feng XT, Guo HS, Yang CX, Li SJ (2018) In situ observation and evaluation of zonal disintegration affected by existing fractures in deep hard rock tunneling. *Eng Geol* 242:1–11. <https://doi.org/10.1016/j.enggeo.2018.05.019>
- Feng XJ, Zhang QM, Liu XF, Ali M (2020) Numerical simulation of the morphological effect of rock joints in the processes of concentrating elastic strain energy: a direct shear study. *Arab J Geosci* 13(7):1–11. <https://doi.org/10.1007/s12517-020-5280-5>
- Huang D, Tan Q, Huang RQ (2012) Mechanism of strain energy conversion process for marble damage and fracture under high stress and rapid unloading. *Chin J Rock Mech Eng* 31(12):2483–2493. <https://doi.org/10.3969/j.issn.1000-6915.2012.12.012> (in Chinese)
- Huang YR, Mao JX, Lin CY (2014) The multi-criteria evaluation of rockburst proneness on deep buried large tunnel. *Chin J Ry Eng Soc* 7:89–94. <https://doi.org/10.3969/j.issn.1006-2106.2014.07.017> (in Chinese)
- Hu L, Feng XT, Xiao YX, Wang R, Feng GL, Yao ZB, Niu WJ, Zhang W (2020) Effects of structural planes on rockburst position with



- respect to tunnel cross-sections: a case study involving a railway tunnel in China. *Bull Eng Geol Environ* 79(2):1061–1081. <https://doi.org/10.1007/s10064-019-01593-0>
- Kuang ZH, Qiu SL, Li SJ et al (2021) A new rock brittleness index based on the characteristics of complete stress-strain behaviors. *Rock Mech and Rock Eng* 54(3):1109–1128. <https://doi.org/10.1007/S00603-020-02311-Z>
- Liu N, Zhang CS, Chu WJ, Ni SH (2017) Discussion on size effect of rockburst risk in deep buried tunnel. *Chin J Rock Mech Eng* 36(10):2514–2521. <https://doi.org/10.13722/j.cnki.jrme.2017.0326> (in Chinese)
- Liu F, Tang C, Ma T, Tang L (2018a) Characterizing rockbursts along a structural plane in a tunnel of the hanjiang-to-weihe river diversion project by microseismic monitoring. *Rock Mech Rock Eng* 52(2). <https://doi.org/10.1007/s00603-018-1649-0>
- Liu XG, Zhang YS, Yu ZF (2018b) Probe into strength characteristics of layered rock based on FLAC3D. *Mining Metall Eng* 38(6):39–47. <https://doi.org/10.3969/j.issn.0253-6099.2018b.06.008> (in Chinese)
- Manouchehrian A, Cai M (2018) Numerical modeling of rockburst near fault zones in deep tunnels. *Tunn Undergr Space Technol* 80(OCT.):164–180. <https://doi.org/10.1016/j.tust.2018.06.015>
- Qiu SL, Feng XT, Zhang CQ (2011) Development and validation of rockburst vulnerability index (RVI) in deep hard rock tunnels. *Chin J Rock Mech Eng* 30(6):1126–1141. (in Chinese)
- Russenes BF (1974) Analysis of rock spalling for tunnels in steep valley sides. Dissertation. Norwegian Institute of Technology
- Sainsbury BA, Kurucuk N (2020) Impact of intact rock properties on proneness to rockbursting *Bull Eng Geol Environ* 8. <https://doi.org/10.1007/s10064-019-01670-4>
- Sepehri M, Apel DB, Adeeb S, Leveille P, Hall RA (2020) Evaluation of mining-induced energy and rockburst prediction at a diamond mine in Canada using a full 3D elastoplastic finite element model *Eng Geol* 266. <https://doi.org/10.1016/j.enggeo.2019.105457>
- Song DZ, Wang EY, Li ZH, Qiu LM, Xu ZY (2017) EMR: An effective method for monitoring and warning of rockburst hazard. *Geomech Eng* 12(1):53–69. <https://doi.org/10.12989/gae.2017.12.1.053>
- Yu Y, Feng XT, Xu CJ, Chen BR, Xiao YX, Feng GL (2020) Spatial fractal structure of microseismic events for different types of rockburst in deeply buried tunnels. *Int J Geomech* 20(4). [https://doi.org/10.1061/\(ASCE\)GM.1943-5622.0001631](https://doi.org/10.1061/(ASCE)GM.1943-5622.0001631)
- Wang CL, Chuai XS, Shi F, Gao AS, Bao TC (2018) Experimental investigation of predicting rockburst using Bayesian model. *Geomech Eng* 15(6):1153–1160. <https://doi.org/10.12989/gae.2018.15.6.1153>
- Wang YL, Xu JM, Xu JS, Zhong CJ (2020) Estimation of rock burst grades using rock mass strength. *Adv Civ Eng*. <https://doi.org/10.1155/2020/2517459>
- Zhao ZN, Feng GL, Feng XT, Chen BR, Xiao YX (2019) Effects of structural planes on the microseismicity associated with rockburst development processes in deep tunnels of the Jinping-II Hydropower Station, China. *Tunn Undergr Space Technol* 84:273–280. <https://doi.org/10.1016/j.tust.2018.11.008>
- Zhang JW, Song ZX, Wang SY (2021) Experimental investigation on permeability and energy evolution characteristics of deep sandstone along a three-stage loading path. *Bull Eng Geol Env* 80(2):1571–1584. <https://doi.org/10.1007/s10064-020-01978-6>
- Zhou J, Li XB, Mitri HS (2018) Evaluation method of rockburst: state-of-the-art literature review. *Tunn Undergr Space Technol* 81:632–659. <https://doi.org/10.1016/j.tust.2018.08.029>